UNIVERSITY OF THE AEGEAN

SCHOOL OF BUSINESS

DEPARTMENT OF FINANCIAL AND MANAGEMENT ENGINEERING

«The effect of graphene nanoplatelets addition on the mechanical performance of epoxy resin»

STUDENT: PARAGKAMIAN ZAFEIROULA

SUPERVISOR: Lecturer ALEXOPOULOS NIKOLAOS

CHIOS, JUNE 2015

This page was left intentionally blank

INDEX

ABSTRACT

Graphene, a single layer of graphite has captured the attention of scientific community due to recently emerging high performance applications. It is considered to be a unique lightweight material with exceptional mechanical and electrical properties. Another interesting material for its good mechanical properties is an important thermosetting polymer, epoxy resin which is widely used in the fields of aerospace, coating, adhesive and electronics. Consequently, high mechanical properties can be achieved with the combination of these two.

The purpose of this thesis is the effect of graphene nanoplatelets addition on the mechanical properties of the resulting polymer nanocomposite. For the preparation of these materials, the system of epoxy resin SR 8100 and hardener SD 8824 was used as the matrix supplied from SICOMIN, FRANCE. Concerning the nanoreinforcement, two types of graphene nanoplatelets (GNPs) were used: Grade C-750 and Grade M-15 with thicknesses 2 and 6 nm, respectively, supplied by XG Sciences, USA. Initially, GNPs were dispersed within epoxy resin using a high speed shear mixer followed by a cure cycle used for this epoxy resin. Following this procedure epoxy nanocomposites were constructed with the concentrations of 0, 0.25, 1, 2, 3, 5 wt% GNPs. The mechanical properties of epoxy/GNPs nanocomposites, such as yield strength, ultimate tensile strength and elongation at fracture were investigated through specific tests and measurements. Fracture toughness tests followed and completed the mechanical test matrix.

The results indicate that the addition of graphene nanoplatelets in epoxy resin results in different mechanical properties that vary regarding the concentration and the type of the GNPs. For the case of Grade C GNPs, tensile strength was increased and the ductility was decreased for low concentrations (< 1 wt% GNPs). For instance, yield strength was increased by 32%, while ductility by 42% with the incorporation of only 0.25wt% GNPs, respectively. On the contrary, for higher GNP concentrations, e.g. 1, 2, 3 wt% strength properties were decreased and ductility were increased, when compared to the respective properties of the neat nanocomposites. For even higher concentrations (> 5 wt% GNPs) there was a decrease for all mechanical properties was observed. Concerning type Grade M GNPs, when their concentration increased, almost all mechanical properties were decreased. Critical stress intensity factor K_{cr} decreased with increasing large (> 1 wt%) GNPs concentration for both investigated types. For instance K_{cr} was reduced for both Grade C with 2wt% GNPs and Grade M with 5wt% GNPs, at 68% and 84% respectively. On the other hand, available literature results showed that a small K_{cr} increase should be expected for very small (< 1 wt%) GNPs concentrations.

ACKNOWLEDGEMENTS

First of all, I would like to thank my Diploma's Thesis Professor and supervisor, Lecturer Nikolaos Alexopoulos for the guidance, encouragement and constant support during my work. Our meetings and discussions made this Thesis possible.

I am especially grateful to Dr. Philippe Poulin for the supply of the materials used in my diploma thesis and his time, at CRPP-CNRS laboratory, at the University of Bordeaux, in France and of course to his co-workers for helping me, advising and allowing me to share the equipment. I enjoyed my stay in Bordeaux and when I was in trouble their patience and comments were really insightful.

I would also like to thank Professor Stavros Kourkoulis for his gratitude to allow us to perform the mechanical tests in the Laboratory of Strength and Materials at National Technical University of Athens and for the fruitful discussions about the mechanical performance of the nanocomposites.

Finally, I am grateful to my parents for the continued support they have given me throughout the period of my work and all the years of my studies. Without their love and support, perhaps this work could not have been carried out.

LIST OF SYMBOLS

Symbol	Unit of Measurement	Definition
L	-	specimen length
F	N	applied forces
A_0	-	initial section of the specimen
E	GPa	modulus of elasticity
R_p	MPa	yield strength
R_m	MPa	ultimate tensile strength
A_f	%	elongation at fracture
A_g	%	uniform elongation
A_t	%	total elongation
R	-	stress ratio
K	-	stress intensity factor
P	N	external load/ axial load
V	mm	the opening of the lips of the specimen
K_{cr}	-	critical stress intensity factor
r	mm	edges opening of toughness specimen
B	mm	toughness specimen thickness
K_R	-	calculating function of the critical stress intensity factor
r_y	mm	plastic area's toughness specimen length
a_{eff}	mm	active length crack
a	mm	crack length
P_{max}	-	maximum axial load imposed in toughness specimen

1. INTRODUCTION

1.1 NANOCOMPOSITES

Nanocomposite is a multiphase solid material where one of the phases has one, two or three dimensions of less than 100 nanometers (nm). They are reported to be the materials of 21st century in the view of possessing design uniqueness and property combinations that are not found in conventional composites. The general understanding of these properties is yet to be reached, even though the first inference on them was reported as early as 1992 [1].

Generally the nanocomposites have many advantages and improved properties. They have improved mehanical properties (tensile strength, stiffness, toughness), dimensional stability, thermal expansion, thermal conductivity and chemical resistance. However there are a few disadvantages associated with the difficulties in dispersion, the increment in viscosity and optical issues.

The properties of the matrix material are significantly affected by the nanoreinforcement. In general, the reinforcement is dispersed into the matrix during processing. A large amount of reinforcement surface area means that a relatively small amount of nanoscale reinforcement can have an observable effect on the macroscale properties of the composite. For example, adding carbon nanotubes improves the electrical and thermal conductivity. Other kinds of nanoparticulates may result in enhanced optical properties, dielectric properties, heat resistance or mechanical properties such as stiffness, strength and resistance to wear and damage.

The mechanical, electrical, thermal, optical, electrochemical, catalytic properties of the nanocomposite differ markedly from the ones of the component materials. In mechanical terms, nanocomposites differ from conventional composite materials due to the exceptionally high surface to volume ratio of the reinforcing phase and/or its exceptionally high aspect ratio. The reinforcing material can be made up of particles (e.g. minerals), sheets (e.g. exfoliated clay stacks) or fibres (e.g. carbon nanotubes or electrospun fibres). The area of the interface between the matrix and reinforcement phase(s) is typically an order of magnitude greater than the one of conventional composite materials [2].

1.2 HISTORY OF NANOCOMPOSITES

Nanocomposites are found in nature, for example in the structure of the abalone shell and bone. The use of nanoparticle-rich materials long predates the understanding of the physical and chemical nature of these materials. The origin of the depth of colour and the resistance to acids and bio-

corrosion of Maya blue paint was investigated attributing it to a nanoparticle mechanism. From the mid-1950s, nanoscale organo-clays have been used to control flow of polymer solutions (e.g. as paint viscosifiers) or the constitution of gels (e.g. as a thickening substance in cosmetics, keeping the preparations in homogeneous form). By the 1970s polymer/clay composites were the topic of textbooks, although the term "nanocomposites" was not in common use [2].

Nanostructured materials have been known and used for decades, even centuries. For instance, nanoparticles were used in the glazes on Ming Dynasty ceramics (1368-1644). Carbon black-reinforced rubber is in use since the early 1900s as a reinforcing agent in automobile tires. These early nanomaterials were produced without the ability to control their structure and morphology, and without a full understanding of what gives nanoparticles their unique properties. In 1959 Richard Feynman said “There’s Plenty of Room at the Bottom” and he described how the laws of physics do not limit the ability to manipulate single atoms and molecules. Instead, it was a lack of the appropriate methods for doing so. The initial commercial nanocomposites were based on nylon. Toyota introduced the first version in the 1980s. It was nylon filled with montmorillonite and used for automobile timing belts. Nylon nanocomposites containing carbon nanotube fillers have come into increasingly widespread use since the 1990s, particularly for applications such as static dissipative components in auto fuel systems, as well as for computer read-write heads. [3].

1.3 APPLICATIONS OF NANOCOMPOSITES

Concerning the applications of nanocomposites, there are many fields that they are used. The number of commercial applications of nanocomposites has been growing at a rapid rate. It has been reported that by 2010, the worldwide production is estimated to exceed 600,000 tonnes and is set to cover the following key areas in the next five to ten years. In automotive (gas tanks, interior and exterior panels), in construction filed (building section and structural panels, in electrical and electronics (electrical components and printed circuit boards), in food packaging (containers and wrapping films) and finally in aerospace (flames retardant panels and high performance components). In aircraft construction the nanocomposites represent an advanced material solution for the structure (stringers, frames) as strengthening element or as skin for the honeycomb structure used at wings and fuselage (Figure 1). These materials are typically lighter and more resistant to corrosion than are the metallic materials that have traditionally been used in airplanes [4].

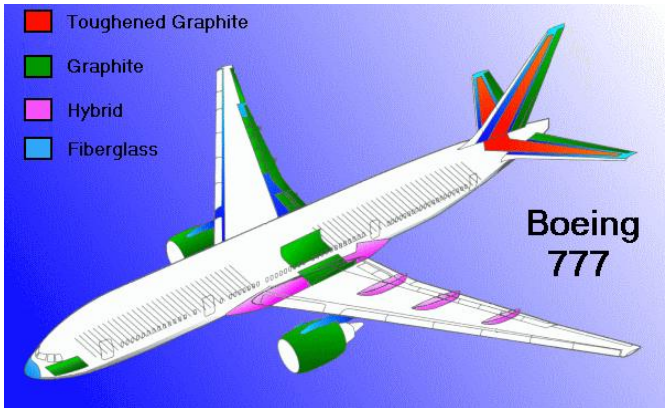

Figure 1: Various nanocomposite and composite materials including graphite are used in structures such as the Boeing 777 [5].

1.4 POLYMERS AND APPLICATIONS

Polymers have a significant role in our life, from our body (proteins, enzymes) and natural goods (wood, rubber, leather and silk) to synthetic ones (useful plastics and fiber materials). Industrially polymers are classified into two main classes – *plastics* and *elastomers*. Plastics which classified in two groups – thermoplasts and thermosets- have a wide range of properties and in most cases they are relatively low in cost. In our project a thermosetting polymer, epoxy resin, will be used. Epoxy resins developed through the 2nd World War and become commercial available around 1950. Due to their properties they have many applications in the industry and one of the most common one is their use as matrices in composites. In addition, epoxy resins are divided to liquid and solid resins. Concerning the liquid resins like ours, they have high mechanical properties and good chemical reaction related to the extras materials and the reinforcement [6].

Each epoxy resin used for the manufacture of composite materials should have the following properties: good mechanical properties, good adhesion properties, good strength properties at fracture, low environmental degradation. Figure 2 shows a typical tensile stress-strain curve of an ideal resin. The diagram indicated high resistance at fracture, high stiffness (which is indicated by the initial slope) and large elongation at fracture. This means that the resin is initially stiff but does not break in a brittle manner.

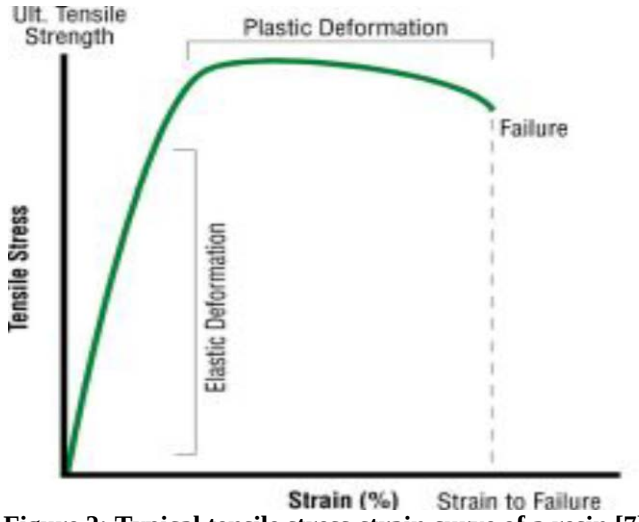

Figure 2: Typical tensile stress-strain curve of a resin [7].

First of all, the wider application of epoxy resin is in the field of paints and coating with good electrical properties and resistance to chemical agents. They are used for corrosion protection of steel pipes, adhesion of marine and automotive paints and for high demand floors. Moreover, epoxy resins are used as adhesives which agglutinate wood, metal, glass and some plastics where high adhesion strength is required (especially for aircraft, automobile). They are also used in industrial production tools and composites (molds, models, laminates, composite materials) and in the field of electrical and electronic systems (engines, generators) protecting electrical components from short circuits. Finally they are used for the repair and the assembly of vessels in marine applications and in aerospace applications they are applied as the material of the structural matrix, which is then reinforced. Figure 3 shows the application of a very strong and flame retardant epoxy (magnobond 92-1) used to reinforce floor panels and wall panels on the Boeing 777 [8].

(a) **(b)**

Figure 3: (a) Different resin applications [9], (b) aerospace applications epoxies as adhesives for the structure [10].

1.5 GRAPHENE AND APPLICATIONS

The last decades we have intense references about a promising nanomaterial graphene, for which the scientific community has shown great interest. Therefore, there is an exponential increase in materials based on graphene as well as the number of its publications. Graphene, the 'mother of all materials reinforced with graphite' as it is called, one of the allotropes (diamond, carbon nanotube, and fullerene) of carbon is a two-dimensional material made from carbon atoms arranged in a honeycomb structure. Moreover it has excellent Young´s modulus ~1 TPa, tensile strength 130 GPa, maximum electrical conductivity over 6000 S/cm, thermal resistance 5000 W/mK and good chemical resistance. It is therefore extremely powerful for its very low weight, and its heat conduct and electricity with high efficiency [11],[12].

We should state that before graphene, carbon nanotubes (CNTs) - that belong to the same family - had a lot of attention and its applications were hundred (Figure 4). However, recent studies though have shown that graphene has a higher ratio of surface volume (better improvement of the mechanical, electrical, thermal and barrier properties of polymer matrix) and is usually cheaper (easily constructed from graphite a raw material in large quantities) than CNTs. More specifically, in this work the type of graphene that had been chosen is the graphene nanoplatelets (GNPs) which are stacks of individual layers of graphite and we will analyze them further below (Figure 5). It is a newly developed material with low cost (available at low cost of $ 5 / lb) and often increases the modulus of the composites [13].

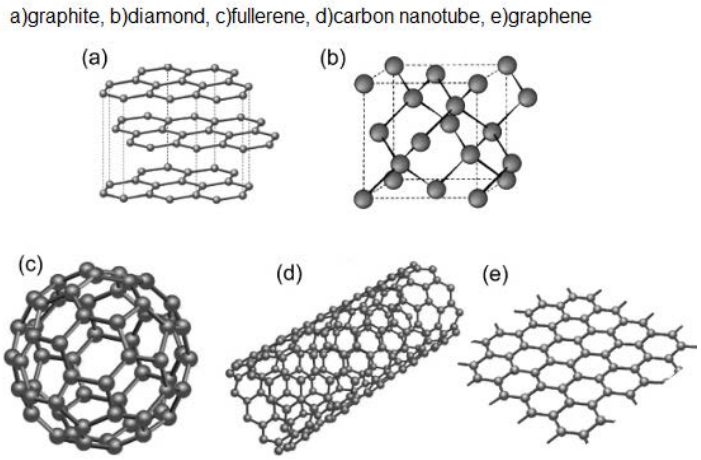

Figure 4: Comparison of graphene with other Carbon materials' [14].

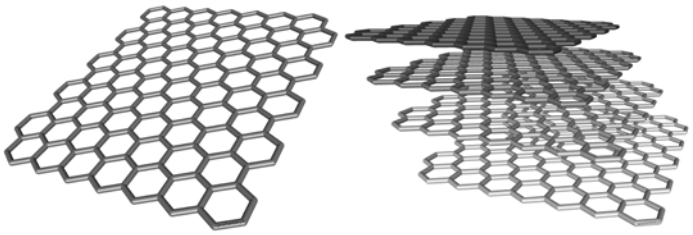

(a) **(b)**

Figure 5: (a) Graphene structure and (b) Graphene nanoplatelets structure [15].

Graphene applications vary as we find them in many fields. First of all we find them in composite materials as reinforcement, for example in sport equipment. Graphene is lightweight and strong so it gives stability strength and flexibility in equipment such as tennis or badminton racquets, baseball bats, racing bicycles, golf clubs and balls, Figure 6. Moreover, in the energy field we find graphene mainly in batteries and in solar cells. Its transparency and conductivity solves two problems of solar cells as light needs a good conductor in order to get converted into usable energy and secondly the cell also has to be transparent for light to get through. In addition, graphene is used in aerospace and marine due to its light weight and finally with a big percentage in semiconductors, electronics and optoelectronics such as in liquid crystal devices, light emitting diodes and electrodes for dye sensitized solar cells.

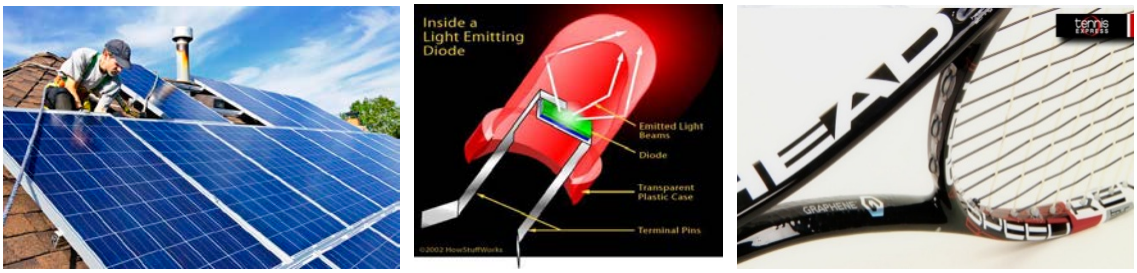

(a) **(b)** **(c)**

Figure 6: Graphene applications: (a) graphene in solar cells, (b) graphene in electronics and (c) graphene in head tennis racquet [16].

1.6 GRAPHENE EFFECT IN MECHANICAL BEHAVIOUR OF COMPOSITE MATERIALS

The exceptional mechanical, chemical and physical properties of graphene in combination with the respective powerful properties of polymers contribute to the development of significant nanocomposites. As a result these composite materials are the best solution in applications where high mechanical materials are required. It should be noticed that although the addition of graphene and the specific amount of it in composites usually increases the elasticity and the tensile modulus, there are other factors that influence the mechanical properties. The dispersion in nanomaterials is a well known challenge because of the issues associated with agglomeration and lack of interfacial

interactions with polymers. Graphene tends to agglomerate due to Van der Waals attraction and its large surfaces, and the additional binding pp- interactions enhance the stacking of graphene sheets. However, more and more researchers interest about graphene and its effect in mechanical properties of composites. As a result as proved through many scientific articles and publications graphene improves the tensile strength, the high modulus, strengthens the capacity erosion, increases the impact strength and finally maintains or improves the ductility of nanocomposites.

1.7 LITERATURE REVIEW

In this section, a literature review is attempted to present the available articles on the mechanical properties of polymer-graphene composite materials.

J. King et al [12] studied the mechanical properties of epoxy/GNPs composites. The materials used were GNPs of thickness 7 nm, the epoxy resin EPON 862 and the Curing Agent W EPIKURE (always used 26.4 g Curing Agent W added to 100 g EPON 862). In addition, a Ross high-shear mixer was used for stirring and the concentrations given were 1-6 wt% GNPs. Macroscopic results showed that tensile modulus was increased up to 23 % and tensile strength and strain were decreased steadily until 54 % and 81%, respectively.

Chatterjee et al [17] investigated the influence of reinforcements on the mechanical and thermal properties of epoxy/graphene nanoplatelets composites. Epoxy resin containing 0.1, 0.5, 1.0, 1.5 and 2.0 wt% EGNPs (expanded graphene nanoplatelets) were processed and characterized prior to subsequent studies. They used 100 g of epoxy resin EPIKOTE 8282VEL and 24 g EPIKURE 3402 as a curing agent. They have used a high-pressure processor followed by three roll milling. The results showed that the hardness and the modulus of the composites increased steadily up to 8.2% and 8.5% respectively with the amount of 1.5 wt% GNPs and then decreased with with higher concentrations. The fracture toughness was increased by up to 66% at 0.1 wt% and then decreased at higher concentrations.

B. Ahmadi et al [18] investigated the mechanical response of epoxy/graphene composites. The materials used were epoxy resin LY564, hardener Aradur 2954 and GNPs of thickness 7 nm. An established method used the three-roll mill with different GNP weight contents (0.25, 0.5 and 1 wt%). Elastic modulus increased steadily and ultimate strength increased with a peak at 0.5 wt% GNPs. Fracture toughness finally was increased by an average of 58% by the addition of 0.25 wt% GNPs.

According to M. Shen et al [19], GNPs were used to reinforce epoxy composite and epoxy/carbon

fiber composite laminates to enhance their mechanical properties. In this study, various amounts of graphene nanoplatelets (with a thickness of 5–25 nm) were uniformly dispersed in epoxy resin (0.25, 0.5, 1, and 1.5 wt% GNPs) and prepared the epoxy nanocomposites. Mechanical properties of the nanocomposite, including ultimate tensile, flexural strength, and flexural modulus, were investigated. As a result with the addition of 0.25 wt% GNPs in the composite there was an increase in tensile strength up to 20% and in flexural strength up to 9%. Moreover at 0.25 wt% GNPs the fatigue life was extended. The flexural modulus finally increased as the amount of GNPs increased and reached a 12% increment.

Q. Meng et al [20], present a low cost processing technique for producing modified GNPs and an investigation of the electrical and mechanical properties of the resulting composites. Two type of GNPs were studied, modified (m-GNPs) and unmodified (unm-GNPs) at the amount of 0.12, 0.25, 0.5, 1 vol % at the epoxy/GNPs composites. The results showed that the Young's modulus increases steadily, with 1 vol% GNPs they had 24% increment for m-GNPs which was 8% higher increment than unm-GNPs. The tensile strength on the other hand decreases steadily, with 0.25 vol% GNPs they had 14.5 % decrement for m-GNPs and 18.2 % decrement for unm-GNPs. At 0.1 vol% the decrement in tensile strength was 40%. In addition, fracture toughness and energy increased until reaching peak values at 0.25-0.50 vol% and then started to decline. For 0.25 vol% fracture toughness increased 188 % for m-GNPs and 136 % for unm-GNPs.

M. Naebe et al [11], produced thermally reduced graphene nanoplatelets functionalised via Bingel reaction to improve their dispersion and interfacial bonding with epoxy resin 862 and curing agent EPIKURE W (always used 100 g resin to 26,4 g curing agent). Nanocomposites containing a small functionalised graphene loading (0.1 wt%) with the use of an ultrasonication and the appropriate procedure demonstrate improvement 22% in flexural strength and 18% in modulus. The improved mechanical properties of nanocomposites is due to the uniform dispersion of functionalized graphene and strong interfacial bonding between modified graphene and epoxy resin as confirmed by microscopy observations.

According to S. Saw et al [21], epoxy composites with nanoparticles (synthetic diamond and graphene nanoplatelets) were prepared (0.5, 1, 1.5, 2 vol% GNPs) and characterized based on tensile, thermal, and electrical properties. In this work, ultrasonic agitation method was used for mixing of epoxy resin EPON Resin 8,281 and nanoparticles and curing agent Polyetheramine D230 was added at a ratio of 100:32 by weight (epoxy: curing agent).The results showed increment in thermal conductivity and electrical conductivity but decrement in elastic modulus, tensile strength,

elaongation at break and storage modulus (because of the formation of large agglomerations). With incorporation of GNPs there was decrement in elastic modulus, especially with 0.5 vol% GNPs there was 36.84% decrement. In addition, the tensile strength decreased 62.22% with the amount of 1 vol% GNPs.

According to J. Ma et al [22], epoxy/GNPs composites were produced to investigate their mechanical properties. Modified 3-nm thick graphene platelets were mechanically mixing and sonicating into epoxy (DGEBA, Araldite-F). The concentrations of GNPs in the composites were 0, 0.32, 0.98, 2 vol% and the following results concern the amount of 0.98 vol%. There was a steadily increment in Young's modulus 14.2% for m-GNPs and 9.72% for unm-GNPs and on the other hand a steadily decrement in tensile strength 16 % for m-GNPs and 38 % for unm-GNPs. The toughness was increased for this amount of GNPs 134 % for m-GNPs and 69.7% for unm-GNPs.

S. Chandrasekaran et al [23], prepared and characterized the GNP/epoxy nanocomposites and investigated their mechanical response. Epoxy Araldite LY556 nano-composites were prepared by dispersing GNPs using two different techniques: three-roll mill (3RM) and sonication combined with high speed shear mixing (Soni_hsm). The concentrations used were 0.3, 0.5, 1, 2 wt% GNPs. The toughening effect of GNPs was most significant at 1.0 wt% loading, where a 43 % increase in K_c was observed. Among the two different dispersion techniques, 3RM process gives the optimum dispersion where both electrical and mechanical properties are better.

Y. Zhang et al [24], discussed about a strategy for covalent functionalization of graphene platelets and unmodified GNPs and the fabrication of their composites with epoxy resin. Epoxy resin of commercial grade Epon44 and 0.1, 0.3, 0.5 wt% GNPs were used. As a consequence of the good dispersion state of GNPs in matrix, and the covalent interactions between GNPs and epoxy, significantly improved Young's modulus (16 %), tensile strength (14 %) and fracture toughness (27 %) as compared to neat epoxy. The improvements were even larger for f-GNPs.

According to MM Shokrieh et al [25], graphene nanoplatelets are used to improve the static and fatigue flexural stiffness and strength of epoxy resin. Epoxy ML-526 (Bisphenol-A), curing agent HA-11 (polyamine) and GNPs (0.05, 0.1, 0.25, 0.5, 1 wt%) of thickness 3-5 nm were used. Maximum improvement on flexural modulus was obtained at 0.25% of graphene content and it is increased by 13 % and maximum improvement on flexural strength was obtained at 0.1% of graphene content with an increment of 8.18%.

According to F. Wang et al [26], in this study investigated the influence of GNP sizes and

dispersion on the mechanical and thermal properties of epoxy nanocomposites. Two types of GNPs GnP-C750 and GnP-5 were sonicated in the epoxy matrix. The mechanical property measurements showed that larger nanoplatelets (GnP-5) exhibited greater reinforcement in improving the modulus of the composites compared to GnP-C750. As a result for using type GnP-5 there was a decrement at 5 wt% GNPs by 37 % on tensile strength and an increment in modulus by almost 26 %.

Table 1: Mechanical properties of Epoxy resin/Graphene Nanoplatelets composites

RESIN	GNPS THICKNESS (NM)	GNPS CONCENTRATION		MODULUS (%)	TENSILE STRENGTH (%)	FRACTURE TOUGHNESS (%)	REF
		wt %	vol %				
EPON 862	7	0, 1, 2, 3, 4, 5, 6		23.52 ↑	54.25 ↓	-	12
Epikote 8282VEL	-	0, 0.1, 0.5, 1, 1.5, 2		8.2 ↑	8.5 ↑	66 ↑	17
EPO 622	5-25	0, 0.25, 0.5, 1, 1.5		19 ↑	20.24 ↑	- ↑	19
EPON 8281	10	0, 0.83, 1.66, 2.5, 3.33	0, 0.5, 1, 1.5, 2	36.84 ↓	62.22 ↓	-	21
Araldite LY564	7	0, 0.25, 0.5, 1		- ↑	- ↑	57.69 ↑	18
EPON 862	-	0, 0.1		18 ↑	22 ↑	-	11
DGEBA Araldite-F	3	0, 0.2, 0.41, 0.83, 1.66	0.12, 0.25, 0.5, 1	15.9 ↑	40 ↓	136.3 ↑	20
DGEBA, Araldite-F	3	0, 0.53, 1.63, 3.33	0, 0.32, 0.98, 2	9.72 ↑	37.8 ↓	69.7 ↑	22
Epon44	-	0, 0.1, 0.3, 0.5		16.66 ↑	14 ↑	27.62 ↑	24
ML-526 Bisphenol-A	3-5	0, 0.05, 0.1, 0.25, 0.5, 1		13.3 ↑	8.18 ↑		25

1.8 MOTIVATION

During the last few decades an important effort on research has been carried out concerning the composite materials reinforced with graphene. This is due to the excellent mechanical properties of graphene. One of the main areas where this material finds application is the aerospace industry as we have already mentioned. In this field of aerospace structures the constant evaluation of the remaining life of the equipment has been decided critical at each stage of their service. Hence, increased tensile mechanical properties are always needed along with increased fracture toughness.

According to the above literature review, research on epoxy/GNPs composites focused mainly on the processes of dispersion of GNPs and the evaluation of their mechanical properties. In this Thesis we will study the effect of GNPs on epoxy tensile mechanical properties and their correlation along with fracture toughness for different types of GNPs as well as GNPs concentrations.

2. EXPERIMENTAL PROCEDURE

The purpose of this section is to describe the methodology, the materials and the experimental series which were carried out for the experimental tests. Two types of experiments were performed. Tensile specimens and fracture toughness specimens were fabricated containing the appropriate amount of GNPs in order to be compared with no GNPs specimens and be analyzed subsequently.

2.1 METHODOLOGY

The approach methodology includes the preparation of tensile specimens and fracture toughness specimens made from resin and GNPs, as shown in Figure 7. The specimens were manufactured with the appropriate materials, dispersed with a high speed mixer and placed into the oven for specific time and temperature. The tensile specimens were subjected to mechanical tensile test according to specification ASTM D638 [27] and their mechanical properties were evaluated. The mechanical toughness tests were performed according to ASTM D5045 [28]. The experimental results of the above mechanical tests were compared with the corresponding available literature experimental data.

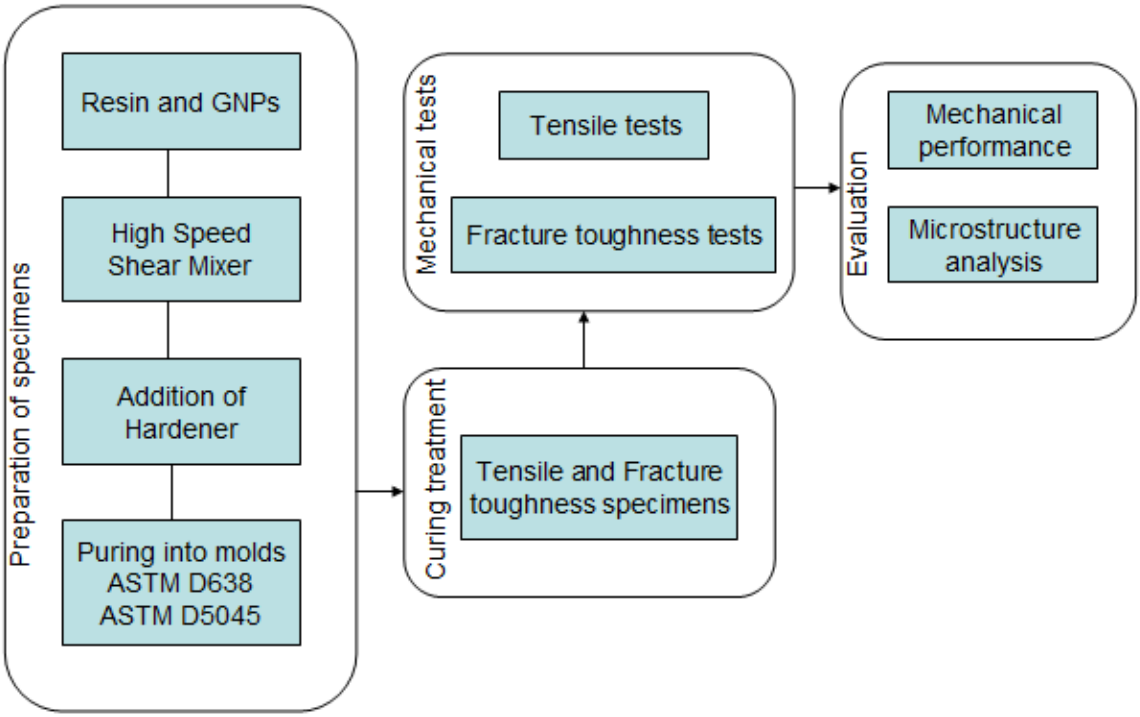

Figure 7: Flow chart of the processing procedure.

2.2 MATERIALS

Two types of GNPs were used in this experimental procedure, supplied by XG Sciences, USA with the commercial names xGnP Grade C-750 and xGnP Grade M-15. The size of a typical Grade C sample has a distribution that ranges from very small flakes (below 100 nm) up to relatively large flakes (1-2 um). More specifically, Grade C-750 has the smallest average size, followed by C-500 while C- 300 has the largest average size and respectively a specific surface area of 300, 500, 750 m^2/g. In this Thesis, the average flake thickness is 2 nm and the average particle diameter is 2 μm. Concerning the second type of GNPs Grade M, particles have an average thickness of approximately 6 nm and a typical surface area of 120 to 150 m^2/g. Grade M is available with average particle diameters of 5, 15 or 25 microns and specifically in this project the 15 μm-diameter particles are used.

The epoxy resin used is the SR 8100 and the hardener is the SD 8824. Exactly 100 g of epoxy resin was added to 22 g of Hardener, Figure 8. The viscosity of SR 8100 and SD 8824 at 20^oC is 930 ± 100 mPas and 8 mPas, respectively. This system supplied from SICOMIN (13161 Chateauneuf Martigue Cedex - France) has very low viscosity at ambient temperature and high mechanical properties can be achieved using the ratio **SR 8100 / SD 8822-24.**

(a) (b) (c) (d)

Figure 8: (a) The three materials that they were used in the experimental procedure, from left to right: resin, graphene, hardener, (b) the graphene in powder form before the dispersion, (c) the yellow-color resin, (d) the transparent-color hardener.

2.3 SPECIMEN FABRICATION

To fabricate the neat epoxy composites - references, 100 g of Epoxy SR 8100 was added to 22 g of hardener SD 8822-24 at room temperature and mixed by hand for 3 min. Then the mixture was poured into the molds and placed in a vacuum heating oven (Salvis Lab VC-20 Vacucentre Vacuum Oven) where vacuum pumping was performed for 10 min at room temperature to eliminate air bubbles. The applied curing treatment was carried out at 60°C for 40 min and then again for post-

curing at 60°C for 4 hours.

To fabricate the epoxy/GNPs composites, the appropriate amounts of GNPs, which will be analyzed below, were added to resin. The materials were mixed using a High Speed Shear Mixer Silverson L4RT at 4000 rpm for 30 min, Figure 9. Next, the appropriate amount of hardener (always used 100 g epoxy resin added to 22 g hardener) was added to the GNPs/resin solution and mixed by hand at room temperature for 3 min. The mixture was poured into the molds, degassed for about 10 min at room temperature under vacuum until it was completely bubble free, as described in the neat epoxy specimens. Then cured at 60°C for 40 min and post-cured at 60°C for 4 hours.

Finally, when the samples were polished by hand (sandpaper type P800 was used) at their lateral surfaces before the mechanical testing.

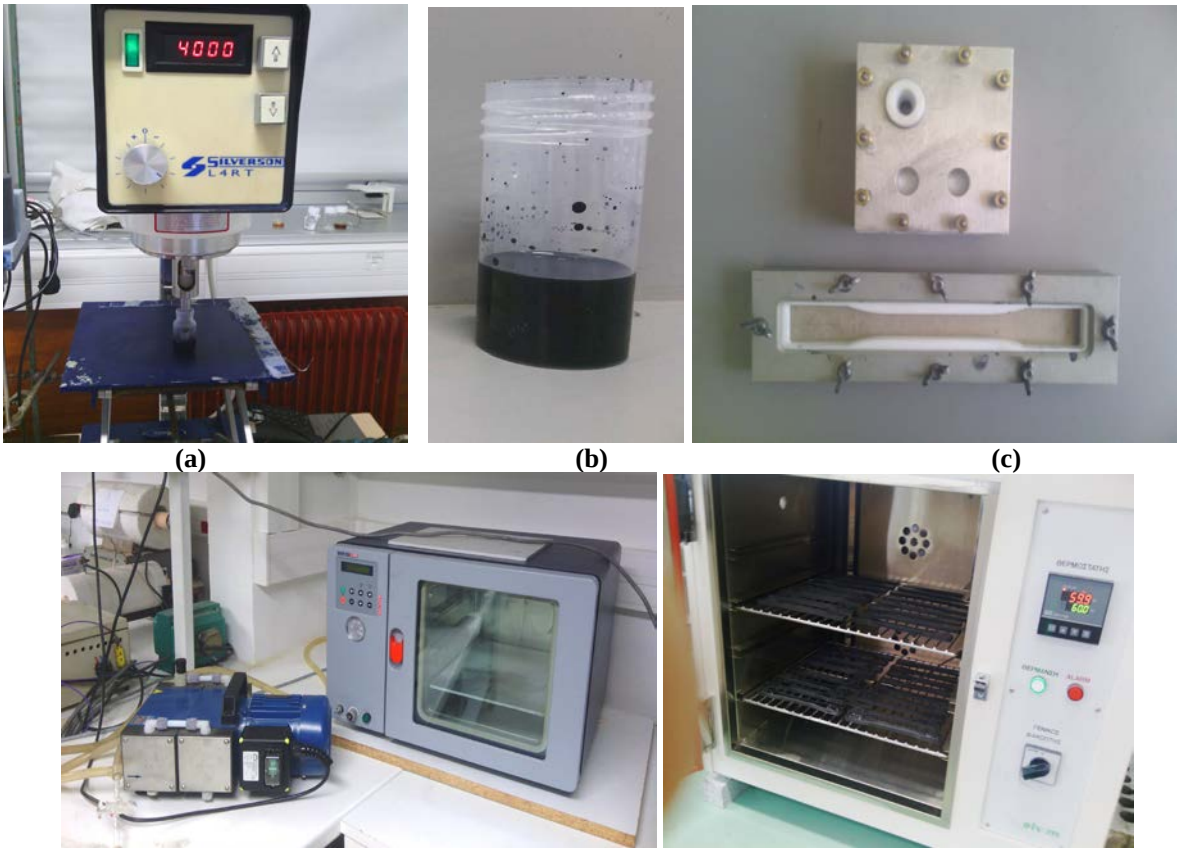

Figure 9: (a) The resin-GNPs mixture during the dispersion process, (b) the final mixture including all materials, resin, GNPs, hardener, (c) tensile mold and fracture toughness mold (d) vacuum oven and vacuum pumping for casting the molds and (e) tensile specimens in the oven for post-curing.

The construction of the molds and the preparation of the composites were performed at the Centre de Recherché Paul Pascal – CNRS, of Bordeaux in France. Initially, the molds were constructed according to the specifications ASTM D638 for tensile tests and ASTM D5045 for fracture

toughness tests, as can be seen in Figures 10 and 11, respectively.

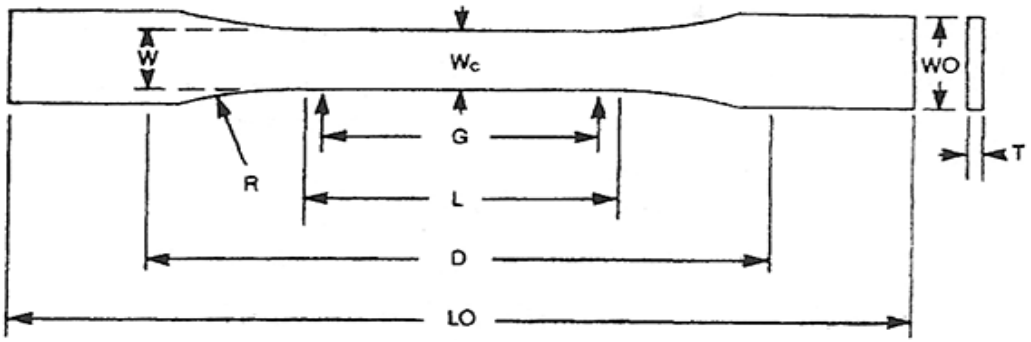

Specimen Dimensions for Thickness, T= 7, mm (in)

W—Width of narrow section	13 (0.50)
L—Length of narrow section	57 (2.25)
WO—Width overall, min	19 (0.75)
LO—Length overall, min	165 (6.5)
G—Gage length	50 (2.00)
D—Distance between grips	115 (4.5)
R—Radius of fillet	76 (3.00)

Figure 10: Mold geometry for tensile according to specification ASTM D638.

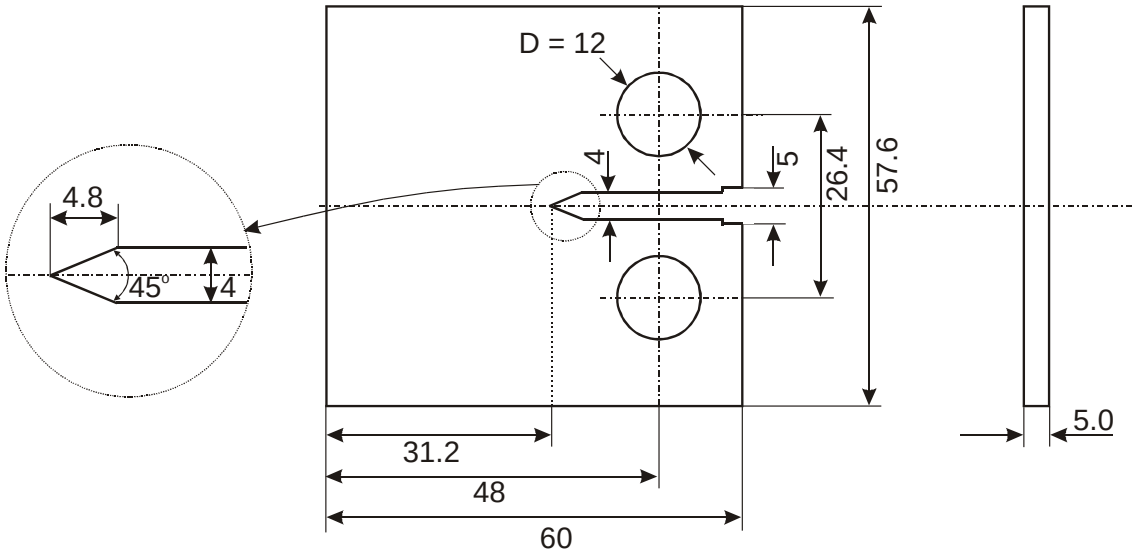

Figure 11: Mold geometry for fracture toughness according to specification ASTM D5045.

In addition, 11 different experimental batches were carried out. One for the neat epoxy samples and ten different for the resin/GNPs composites. For the 2 nm thickness GNPs-Grade C five batches were performed one for each concentration and for 6 nm thickness GNPs-Grade M five batches were also performed, as shown in Table 2. In total 73 samples were produced and experimentally tested.

Table 12: Experimental batches concerning the thickness and the concentration of GNPs.

Total number of specimens: 73.

Thickness of GNPs	Mechanical specimens	Concentration of GNPs					
		0 wt %	0.25 wt %	1 wt %	2 wt %	3 wt %	5 wt %
2 nm	Tensile	4	2	4	5	4	4
	Fracture toughness	3	2	3	4	3	3
6 nm	Tensile	4	2	4	4	4	4
	Fracture toughness	3	2	3	3	3	3

2.4 CHARACTERIZATION

2.4.1 MICROSTRUCTURE

In order to obtain microscopic information of nanocomposites, the materials were characterized using optical microscope and scanning electron microscope (SEM). As can be seen in Figure 12, the samples were placed on a plastic plaque and optically observed. The analysis was carried out in a Leica DMR Optical Microscopy.

Figure 13: Sample testing from the final mixture with optical microscopy.

2.4.2 TENSILE TEST

“Tensile test” is the fundamental material science test in which a sample is subjected to a controlled tension until its fracture. Forces F are applied equal and opposite, acting at the edges of the specimen and along the axis and tend to increase the length, with initial section A_0 and initial length L_0.

A material is considered to be ductile when it has large deformations until its final macroscopic

fracture. The ductile materials can be plastically deformed and save large strain energy densities per unit volume until fracture. Conversely, a material characterized as brittle when it fails immediately when entering the area of plastic deformation, when it gets further from the linear elastic range of the law of Hooke. To carry out a tensile test, a constant displacement rate of grips of the engine is applied at the specimen to cause elongation.

The tensile tests were performed according to the standard ASTM D638, using an MTS Insight electromechanical machine with maximum static load of 10 kN, at the Strength and Materials Laboratory of School of Applied Mathematical and Physical Sciences at the National Technical University of Athens. During the tensile tests, the maximum applied tensile load was 5 kN and the rate of displacement of the tensile machine grips was kept constant and equal to 0,016 mm/min.

(a) **(b)**

Figure 14: (a) Layout of the experimental tensile test and (b) reference tensile specimen in the grips of the tensile machine with the adjusted extensometer recording the reference length.

Initially, the two grips of the machine were aligned in order the specimen can not be twisted and suffer from parasitic bending loads. An Instron extensometer 2620-601 (50 mm gauge length) placed on the reduced section of the specimen, to collect accurate displacement data. During the experiments all the force data, the grips displacement as well as the extensometer's deformation were recorded and stored in a computer. Figure 14 shows a batch of experimental specimen after tensile testing.

Figure 15: A tensile batch (four resin/GNPs specimens) after the conducted experimental procedure.

For the convenience of the reader, the evaluation of the tensile mechanical properties is summarized in Figure 15. Concerning the experimental values of tensile axial load and displacement of the reference length of the specimen, the curve of nominal stress and nominal strain is calculated and the mechanical properties of the specimen can be identified through these.

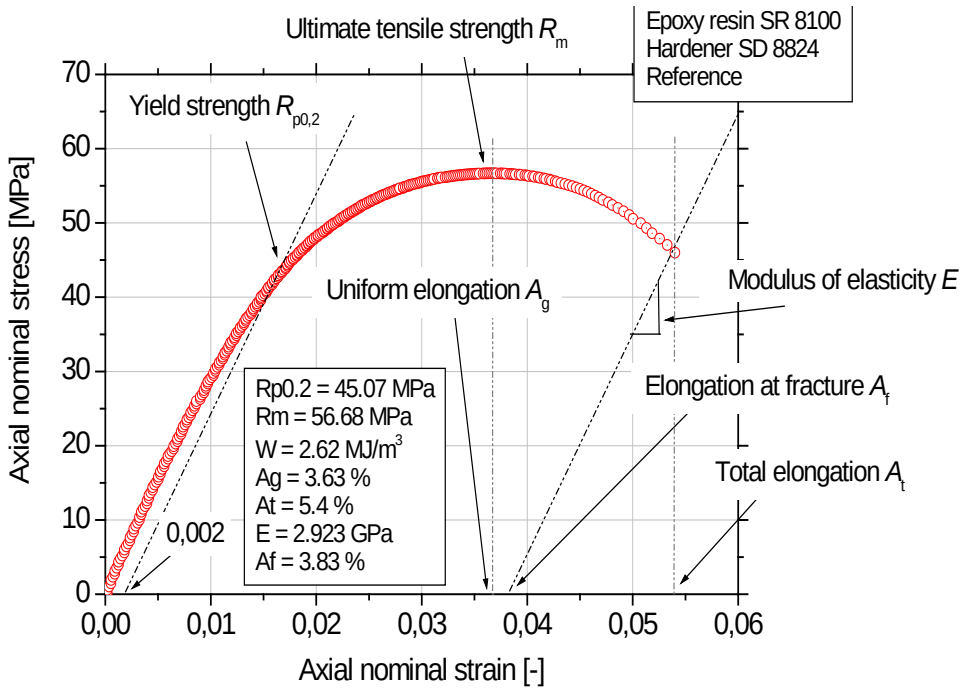

Figure 16: Typical curve of nominal stress-nominal strain.

- Modulus of elasticity (E): It is defined as the slope of the line which is tangential to the nominal stress - nominal strain curve, in the linear elastic range. The modulus of elasticity is measured in GPa.
- Yield strength (R_p): It is defined as the point that irreversible deformations appear.

Something like that means that plastic deformations are created which are not eliminate by removing the applied load. It is measured in MPa. For this project, the yield strength was evaluated by the offset method and the yield strength $R_{p0.2}$ was calculated. According to the specification **[**29**]**, it is measured by bringing the slope of the line from which the modulus of elasticity is calculated at 0.2% of the total nominal deformation of the specimen.

- Ultimate tensile strength (R_m): It is the maximum nominate strength which is developed in the material before it fails due to breakage. It is calculated from the ratio of the maximum tensile load P_{max} to the initial cross section of the material and it is measured in MPa.
- Elongation at fracture (A_f): It is a measure of ductility of the material. It is defined as the ratio of the length change of the measuring area of the specimen, to the original reference length (L_0).

  According to Figure 15 if a parallel line is taken from the break point (the last point of the curve) to the elastic area (linear) of the material, then from the point of intersection of this line with the axis of nominal strain we calculate the elongation at fracture. The elongation at fracture is a dimensionless value (ratio of length to length) and it is usually expressed as percent deformation [%].

- Strain energy density (W): It is the area under the entire tensile nominal stress - nominal strain curve until fracture. Represents the ability of the material to absorb - stores strain energy in its microstructure until the failure and calculated from the completion of the tensile curve. Unit of measure is MJ/m^3.
- Uniform elongation (A_g): Corresponds to the point of the maximum strength and it is the maximum axial elongation that the specimen deforms uniformly. It is usually expressed as a percentage uniform deformation [%].
- Total elongation (A_t): It is the total axial deformation just before macroscopic fracture of the specimen. The total deflection corresponds to the sum of elastic and plastic deformation that has been assigned to the specimen and expressed as a percent total deformation [%] [[30].

There are some useful links below, related to mechanical properties of a material.

By dividing the applied load F with the initial reduced section of the specimen A_0, the stress of the specimen is calculated during the experiment.

$$\sigma = \frac{F}{A_0}, N/mm^2 \quad , \qquad (1)$$

The strain of the specimen (the elongation) is measured at the reduced cross-sectional area and

equals with the ratio of the difference of the displacement to the original length:

$$\varepsilon = \frac{\Delta L}{L_0} \quad , \tag{2}$$

An important measure for evaluating the mechanical properties of a material is the elongation at fracture from which can be distinguished the ductility of the material. It is calculated from the change in the length of the measurement region (reference length) during the tensile test. L_0 is the initial gauge length (reference length-gauge length) and L_f is the final length measurement, resulting from the measurement of the length reference after we put together the two broken pieces of the specimen.

$$\mathrm{A}_f = \frac{L_f - L_0}{L_0} \quad , \tag{3}$$

The ability of the material to store-absorb energy in its microstructure until its failure seems from the strain energy density. The strain energy density W (tensile toughness) is calculated by completing the tensile curve.

$$W = \int_0^{\mathrm{A_T}} \sigma \cdot d\varepsilon, {}^{kJ}\!/_{mm^3} \quad , \tag{4}$$

Finally, another important measure is the modulus of elasticity, which is calculated from the following equation (law of Hooke). The modulus is also calculated from the slope of the diagram stress-strain at the elastic regime of the curve. The proportionality factor E is often called in the literature Young's modulus.

$$\sigma = \mathrm{E} \cdot \varepsilon \Rightarrow \mathrm{E} = \frac{\sigma}{\varepsilon} \quad , \tag{5}$$

2.4.3 FRACTURE TOUGHNESS TEST

Fracture toughness is one of the most important properties in science materials and describes the ability of a material containing a crack in order to resist fracture.

The tests (resistance curve) were conducted using the toughness specimens with a side notch, as can be seen in Figure 11 and performed according to the standard ASTM D5045 in the machine MTS Insight with maximum static load of 10 kN, at the Strength and Materials Laboratory of the School

of Applied Mathematical and Physical Sciences at the National Technical University of Athens. For the tests an appropriate extensometer was used to measure the displacement of the edges of the crack (Crack Opening Displacement, COD) with rate of displacement of the grips constant and equal to 0,001 mm / min, as shown in Figure 16.

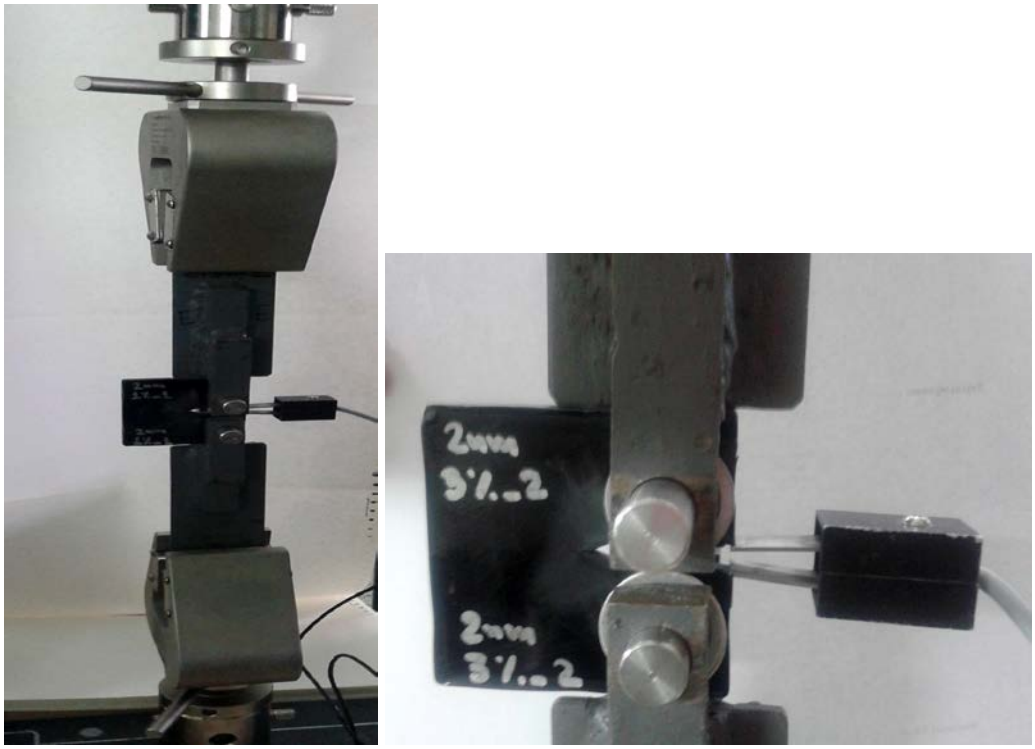

(a) **(b)**

Figure 17: (a) Layout of experimental fracture toughness test with adjusted the extensometer recording the opening of the side edges and (b) zoom with focus on toughness specimen.

The tests were conducted according to the above specification and the following two steps.

1. Pre-crack step

Initially, natural notches were made in the fracture toughness specimens by inserting a fresh razor blade into the existing mold notches The razor cut width was about 1 mm in the midsection of the specimens. Finally, the total notch length of the specimens was between 1.3 mm and 2.00 mm.

2. Quasi-static load step

Before starting the next step of testing the toughness, the extensometer of the opening of the lips of the crack (Crack Mouth Opening Displacement) is adapted on the specimen. The specimen is subjected to tension with very small displacement rate of 0.001 mm/min of the machine grips and according to specification ASTM D5045. Recording of the load and the CMOD extensometer was carried out. Receiving the data of the experimental curve load - displacement of the lips of the crack, the curve of resistance to breakage K_R of material can be constructed using the compliance method.

Then stress intensity curves K of material are calculated for different external load values P. The critical external load, is the one that the calculated stress intensity factor K curve tangent on the K_R material fracture resistance curve. At this point unstable crack propagation is created, and the critical K_{cr} stress intensity factor can be measured, for particular thickness of the material. Figures 17 and 18 show three fracture toughness specimens, before while and after the conducted procedure.

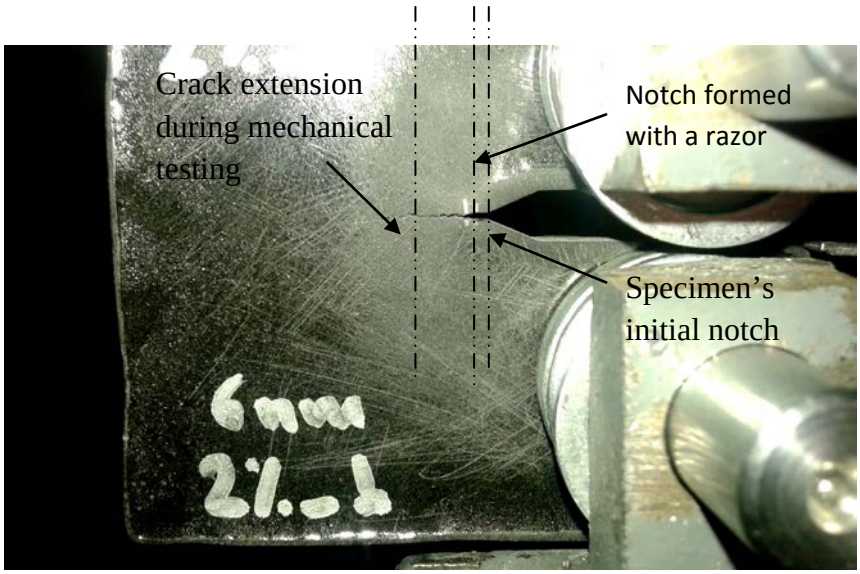

Figure 18: Fracture toughness GNPs/resin specimen during the procedure of quasi-static load step.

(a) **(b)**

Figure 19: Fracture toughness reference specimen before quasi-static load step, (b) the same specimen with a visible crack conducted after the test.

Figure 19 shows the fracture surface of the fracture toughness of GNPs type C and different GNPs concentrations. The bottom that exchibits the rougher surface has 1 wt% GNPs, the just above

bottom has 2 wt% GNPs, the next 3 wt% and the final (top specimen) has 5 wt% GNPs concentrations. It can be noticed that there exist a progressive transition from ductile fracture to brittle. The specimens of this type broke immediately during testing (cleavage fracture) and it was not possible to stop the experiment while the crack progressed. This was not the case for the Grade M GNPs specimens that exhibit lower values of axial load before fracture and presented a visible crack before the crack progression.

Figure 20: Fracture toughness specimens' surface areas after the experiment.

The elaboration of experimental data was performed according to the specification ASTM D5045 to determine the critical stress intensity factor K_{cr}. The process for manufacturing a toughness curve and the graphic determination of the critical stress intensity factor is described below. Originally the quotient C is calculated:

$$C = \frac{V}{P}, \tag{6}$$

where V is the opening of the lips of the specimen and P is the axial load on the specimen. Then the multiplication EBC is calculated by:

$$EBC = E \cdot B \cdot C, \tag{7}$$

where E is the modulus of elasticity of the material which has been calculated from the tensile test specimens of the same experimental batch, and B is the thickness of the test specimens. After the quotient U is calculated:

$$U = \frac{1}{1+\sqrt{E \cdot B \cdot C}}, \tag{8}$$

Immediately after using the calculated U and costants c_0 to c_5 for specimen with side crack type

C(T) on the lips of the crack in which V_0 is given by the following polynomial given in specification ASTM D5045. As shown in Figure 20 the apparent crack length values are calculated to apparent specimen length values *a/w* :

$$a/w = c_0 + c_1 \cdot (U) + c_2 (U)^2 + c_3 \cdot (U)^3 + c_4 \cdot (U)^4 + c_5 \cdot (U)^5 , \quad (9)$$

where a is the crack length of plastic zone measured from the load line and where w is the special charging length of the sample measured by the load line and finally c_0 = 1.0010, c_1 = -4.6695, c_2 = 18.460, c_3 = -236.82, c_4 = 1214.9 and c_5 = -2143.6 for the specific loading / measurement chosen.

$$a/W = C_0 + C_1(U) + C_2(U)^2 + C_3(U)^3 + C_4(U)^4 + C_5(U)^5$$
$$U = 1/[(EBv/P)^{1/2} + 1]$$

	C_0	C_1	C_2	C_3	C_4	C_5
C(T) at V_1	+1.0008	−4.4473	+15.400	−180.55	+870.92	−1411.3
C(T) at V_0	+1.0010	−4.6695	+18.460	−236.82	+1214.9	−2143.6

Figure 21: Values for the constants c_0 to c_5 according to specification ASTM D5045 [30].

Then the polynomial correlation crack length with special length is calculated:

$$f(a/w) = [(2 + a/w)/(1 - a/w)^{3/2}] \cdot [0{,}886 + 4{,}64 \cdot (a/w) - 13{,}32 \cdot (a/w)^2 + 14{,}72 \cdot (a/w)^3 - 5{,}6 \cdot (a/w)^4], \quad (10)$$

By the use of $f(a/w)$ the function of stress intensity factor for different lengths of active cracks is calculated:

$$K_R = (P/B \cdot \sqrt{W}) \cdot f(a/w) , \quad (11)$$

The length of the plastic zone r_y is calculated versus yield strength R_p :

$$r_y = (1/2\pi)(K_R^2 / R_p^2) , \quad (12)$$

Finally, using the above equation, the active length crack a_{eff} is calculated as a function of the initial crack length, the apparent growth rate of the crack, corrected with the length of the plastic zone in front of the tip of the crack:

$$a_{eff} = a_0 + f(a/w) + r_y , \quad (13)$$

Keeping in mind the value pairs *of* K_R and a_{eff} the resistance curve is plotted in Figure 21 for each toughness specimen. Analytical (theoretical) solution of stress intensity factor for the crack length for different axial loads is then calculated. Then, with reference to the maximum axial load value which was imposed on specimen P_{max} and gradually reducing the value of the type *f (a/w),* the curve that abuts on the experimental curve is calculated. The specification states that in this intersection unstable crack propagation is performed, where the critical stress intensity factor K_{cr} for the material and the specific geometry of the specimen is measured. So this is actually a graphical method to calculate the material's critical stress intensity factor K_{cr}.

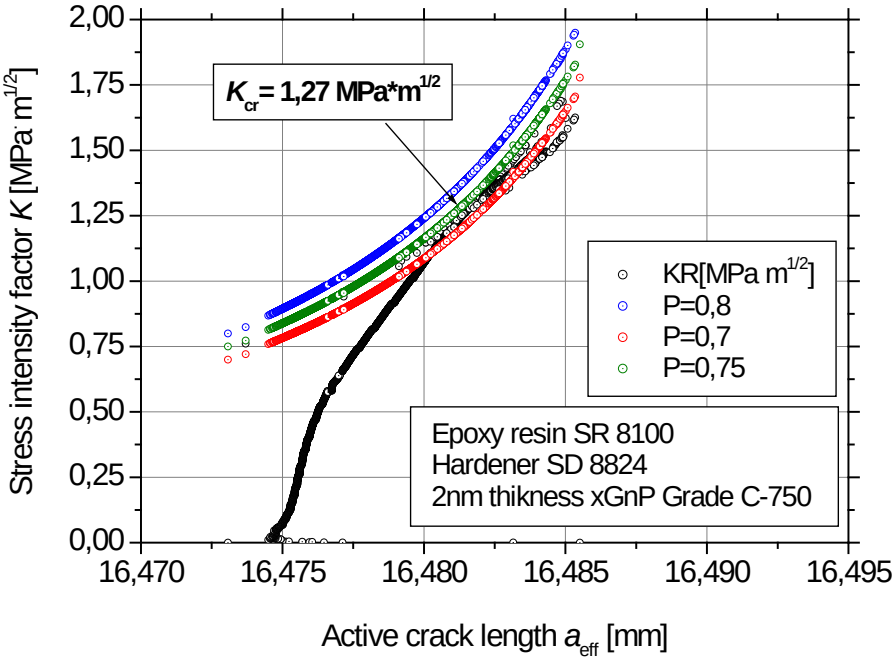

Figure 22 Typical calibration curve of the critical stress intensity factor K_{cr}.

3 EXPERIMENTAL RESULTS

This section presents the experimental results of tensile mechanical properties and fracture toughness tests described in the previous section. These results will be used subsequently to extract conclusions about the effect of incorporation of GNPs on the material's mechanical properties.

3.1 DISPERSION

Nanofiller dispersion is an important issue as GNPs have a tendency to form agglomerates due to strong van der Waals attraction, large surface areas and p–p interaction. With the increase in nanofiller concentration the dispersion becomes even more challenging. The literature review showed that the increase in GNPs content forms agglomeration sites in the composites. This also explains the limitation in improvement in the mechanical properties with increase in nanofiller content [15].

3.2 MICROSTRUCTURE EVALUATION

As already mentioned, the achievement of a good dispersion gives the opportunity to achieve higher mechanical properties. Images in Figure 22 show the random dispersions of 2 nm thickness GNPs-Grade C and 6 nm thickness GNPs- Grade M at the same concentration of 2 wt% GNPs into the resin, respectively. Comparing the two microscope pictures it is obvious that better dispersion was achieved using GNPs Grade C.

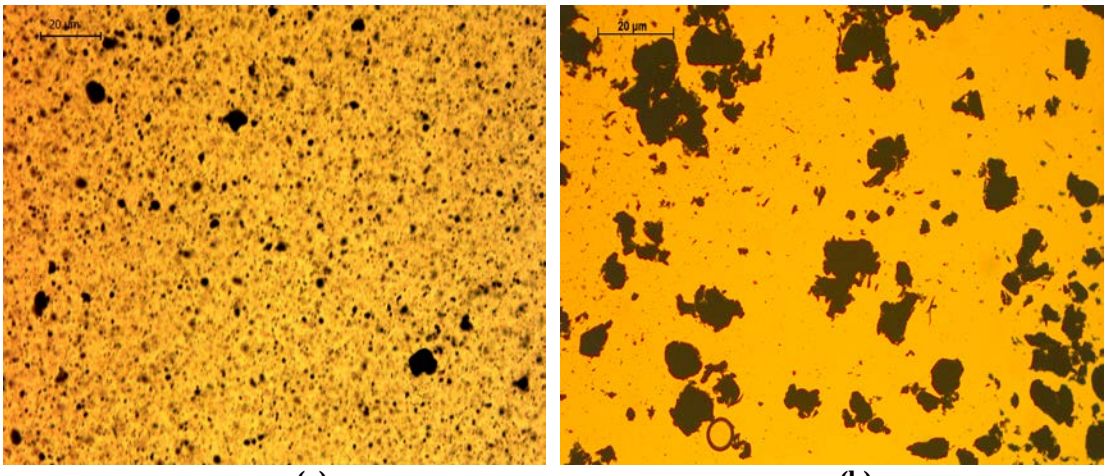

(a) **(b)**

Figure 23: Microscope photograph of 2 wt% GNPs dispersed into the resin (a) Grade C and (b) Grade M.

Figure 23 shows the SEM images with different magnifications, of 2 wt% GNP C-750 and GNPs M-15 comparing with neat epoxy. The presence of graphene nanoplatelets make the interface much

more rough and the differences are clear. The roughness is greater with the 6 nm (Grade M) particles but with a less dense distribution of inhomogeneities compared with the 2 nm (Grade C) particles which were much more homogeneously dispersed.

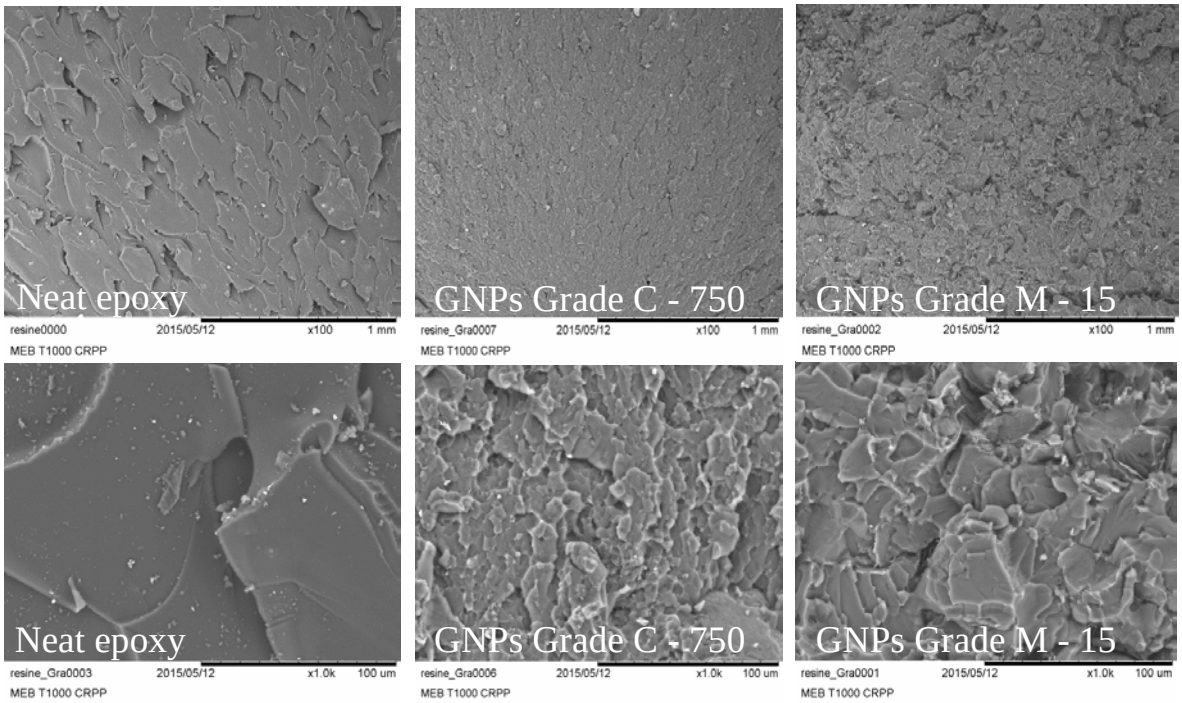

Figure 24: Scanning electron microscopic images of 2 wt% GNPs epoxy nanocomposites with different magnifications.

3.3 TENSILE RESULTS

The results of the tensile tests were used for the tensile curves. The experimental data plotted, in which the x - axis representing the axial strain (linear scale) while the y – axis representing the axial stress (linear scale).

3.3.1 REPRESENTATIVE TENSILE CURVES

Representative curves of nominal axial tensile stress – strain for resin/GNPs Grade C composites are presented in Figure 24. As shown in the diagram the addition of Grade C GNPs increased the strength and decrease the ductility for the low concentrations (< 1 wt% GNPs) while decreased the strength and increased the ductility for even higher concentrations (up to 3 wt% GNPs). For excess reinforcement (> 5 wt% GNPs) all mechanical properties were decreased.

In Figure 25, the corresponding curves are presented for resin/GNPs Grade M composites. The addition of Grade M GNPs increased strength and decrease ductility for the low concentrations (< 1 wt% GNPs) while all mechanical properties for excess reinforcement (> 1 wt% GNPs) were decreased.

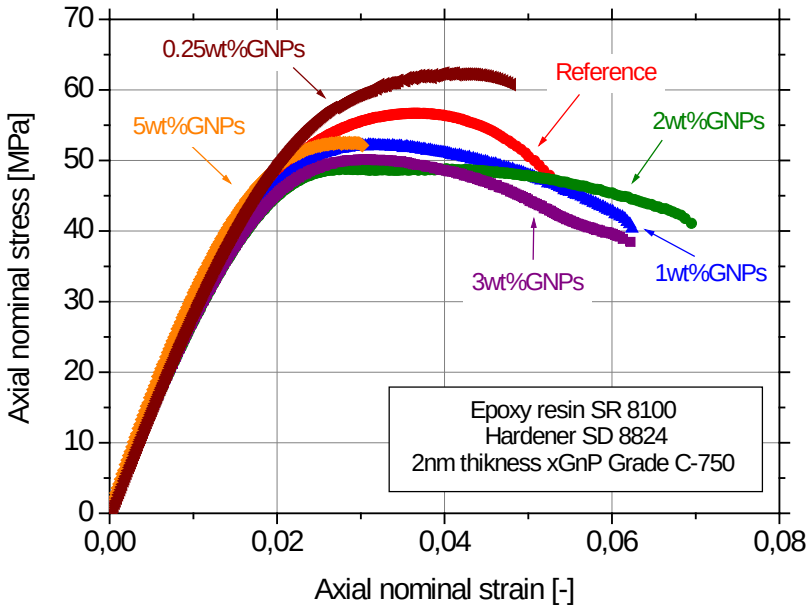

Figure25: Typical tensile curves for GNPs-Grade C and resin composites for 4 different percentages of GNPs.

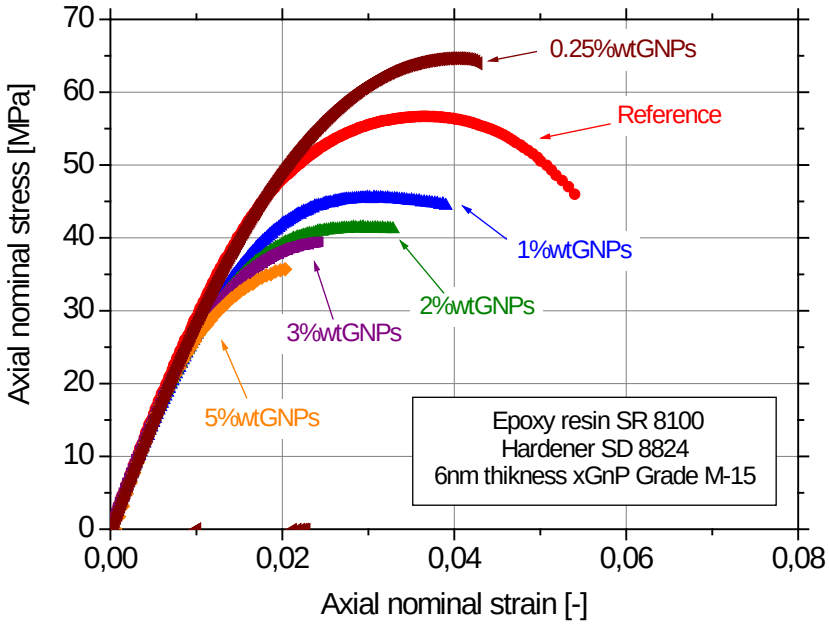

Figure26: Typical tensile curves for GNPs-Grade M and resin composites for 4 different percentages of graphene.

Tables 3 and 4 shows the summarized tensile and fracture toughness results in tabular form with average values and respective standard deviation for the two different GNP types as a reinforcement.

Table 3: Grade C GNPs concentration in epoxy matrix and tensile test results according to ASTM D638 and ASTM D5045 standards.

GNPs (wt %)	Modulus of elasticity E (GPa)	Yield strength $R_{p0.2\%}$ (MPa)	Ultimate tensile Strength R_m (MPa)	Elongation at fracture A_f (%)	Critical stress intensity factor K_{cr} (MPa$\sqrt{m}$)
0.0	2.638 ± 0.05	43.13 ± 0.89	55.87 ± 0.90	4.54 ± 0.62	1.28 ± 0.02
0.25	2.877±0.20	44.53±0.11	62.37 ±0.51	2.63±0.51	-
1.0	2.639 ± 0.01	42.7 ± 0.22	50.69 ± 0.89	5.39 ± 0.85	1.01 ± 0.13
2.0	2.647 ± 0.05	42.1 ± 0.81	48.99 ± 1.67	5.71 ± 0.43	0.42 ± 0.04
3.0	2.777 ± 0.05	42.8 ± 0.11	50.66 ± 0.65	6.41 ± 1	0.49 ± 0.02
5.0	2.895 ± 0.19	43.1 ± 1.31	51.59 ± 1.84	5.04 ± 0.53	0.47 ± 0.05

Table 4: Grade M GNPs concentration in epoxy matrix and tensile test results according to ASTM D638 and ASTM D5045 standards.

GNPs (wt %)	Modulus of elasticity E (GPa)	Yield strength $R_{p0.2\%}$ (MPa)	Ultimate tensile Strength R_m (MPa)	Elongation at fracture A_f (%)	Critical stress intensity factor K_{cr} (MPa$\sqrt{m}$)
0.0	2.638± 0.05	43.13 ± 0.89	55.87 ± 0.90	4.54 ± 0.62	1.28 ± 0.02
0.25	2.812±0.12	45.32±0.51	64.65 ±0.71	1.99±0.53	-
1.0	2.667 ± 0.17	38.1±0.31	45.18 ± 0.35	2.16 ± 0.46	0.30 ± 0.01
2.0	2.681 ± 0.06	35.2 ± 0.42	40.99 ± 0.56	1.55 ± 0.56	0.23 ± 0.06
3.0	2.598 ± 0.02	34.1 ± 0.32	38.16 ± 1.02	0.96 ± 0.15	0.25 ± 0.04
5.0	2.792 ± 0.15	32.1 ± 0.6	35.54 ± 1.55	0.72 ± 0.16	0.20 ± 0.01

3.3.2 YIELD STRENGTH

Figure 26 shows the yield strength $R_{0,2\%}$ for specimens which were constructed from two different types of GNPs. As the chart shows there is a slight $R_{p0.2\%}$ increase is noticed for both GNPs types for the low concentrations (< 1 wt% GNPs). Yield strength of Grade C is not strongly influenced with increasing GNPs concentration, while $R_{p0.2\%}$ continuously decreases for the Grade M

nanocomposites.

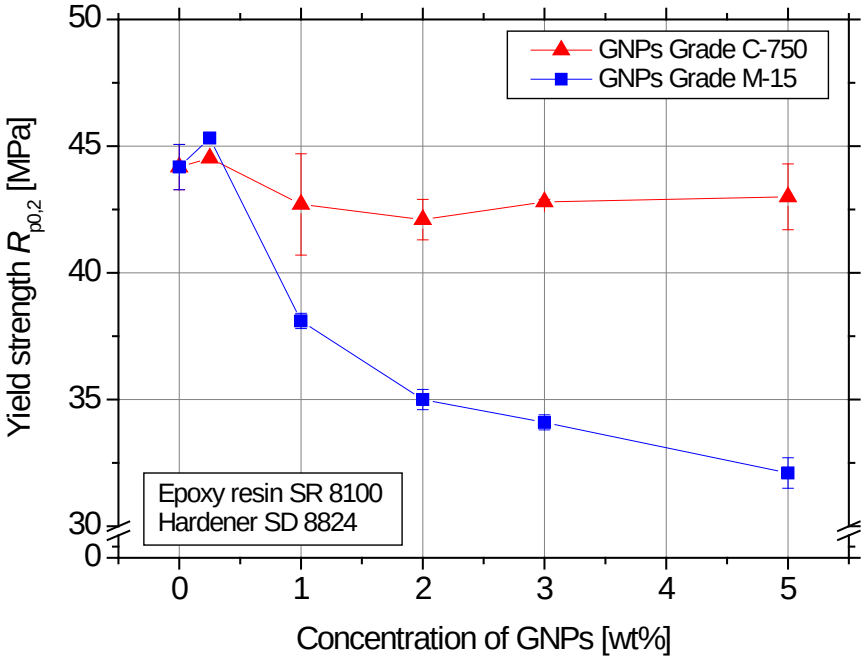

Figure27: Yield strength for the different GNPs types and concentrations.

3.3.3 ULTIMATE TENSILE STRENGTH

Figure 27 shows the ultimate tensile strength results for the different GNPs types and concentrations. Similar results of ultimate tensile strength were drawn from the literature for similar resins and GNPs concentrations.

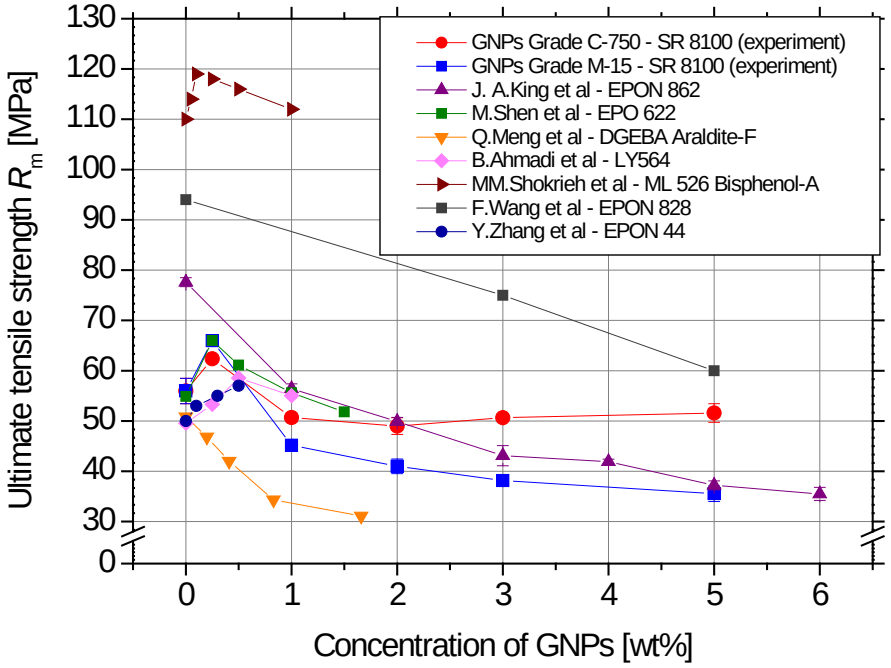

Figure 28: Ultimate tensile strength for the different GNPs types and concentrations.

3.3.4 ELONGATION AT FRACTURE

Figure 28 shows the results of elongation at fracture according to the concentration of GNPs, which ranges from almost 0.7 % to 6.4 % for different types of GNPs and different concentrations. A decrease in ductility is noticed for both types for low reinforcement (<1 wt% GNPs). An enhancement of the ductility for higher concentrations of Grade C GNPs was observed while there was a continuous ductility decrease with increasing GNPs concentration of Grade M. The latter was possibly due to formed porosity, Figure 29.

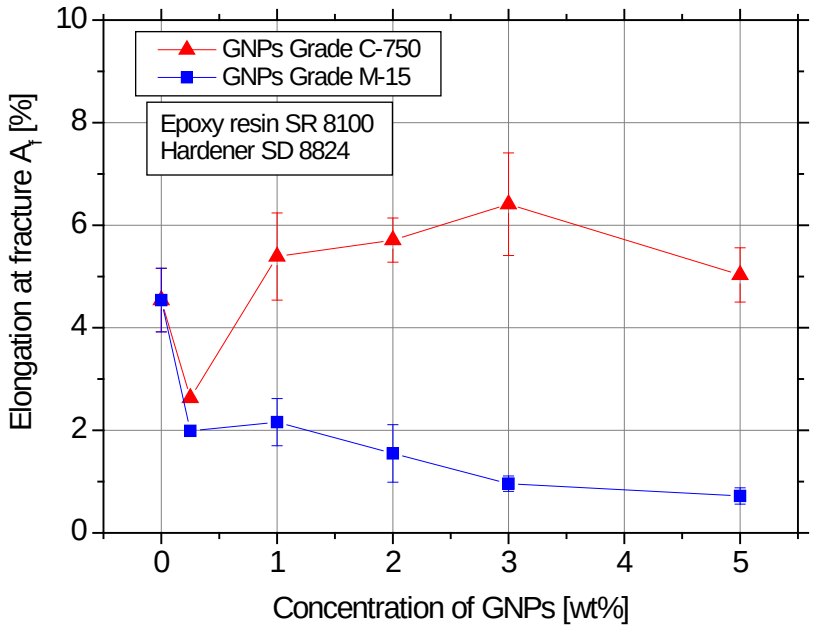

Figure 28: Elongation at fracture for the different GNPs types and concentrations.

Figure 29: Epoxy nanocomposite with 5 wt% incorporation of GNPs showing bubbles in the surface.

3.3.5 MODULUS OF ELASTICITY

Figure 30 shows that modulus of elasticity is increasing with increasing GNPs concentration in the matrix. In addition open literature data confirms our experimental results.

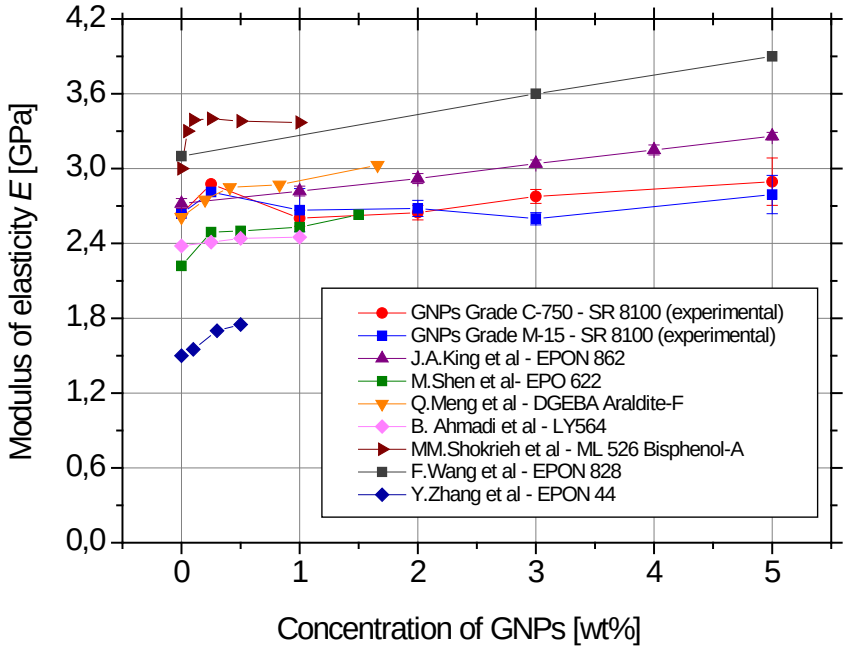

Figure29: Modulus of elasticity for the different GNPs types and concentrations.

3.4 FRACTURE TOUGHNESS RESULTS

Representative curves force - displacement of the edges of the crack for resin/GNPs Grade C and resin/GNPs Grade M composites are presented in Figure 31 and Figure 32 respectively. With the addition of Grade C GNPs cleavage fracture was noticed for higher concentrations (> 1 wt% GNPs). Fracture occurred during the transition from the elastic to the elasto-plastic regime. On the contrary lower concentrations will be examined in the near future. With the addition of Grade M GNPs essential decrease of the maximum load of the R-curve is noticed for all concentrations and lower concentrations (< 1wt% GNPs) will be examined in the near future.

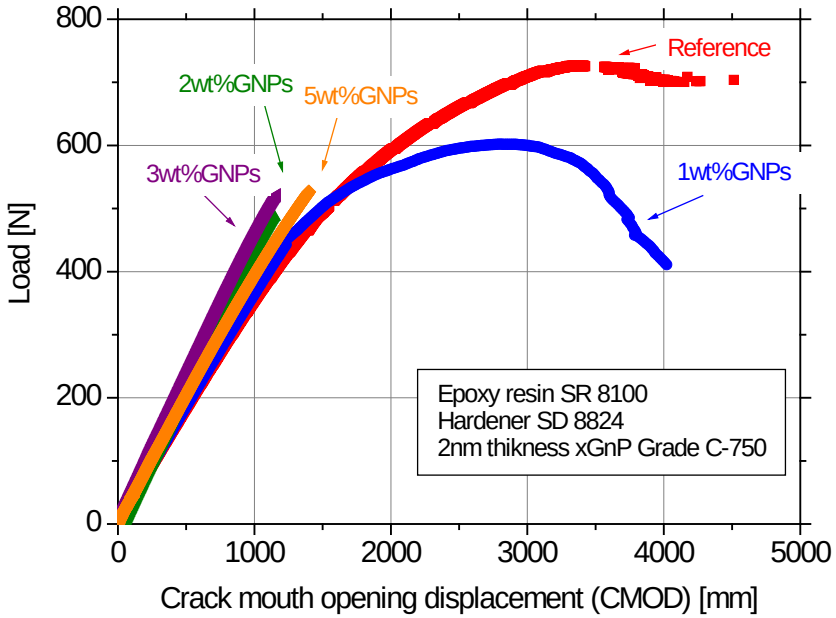

Figure30: Representative curves force - CMOD for resin/GNPs Grade C nanocomposites.

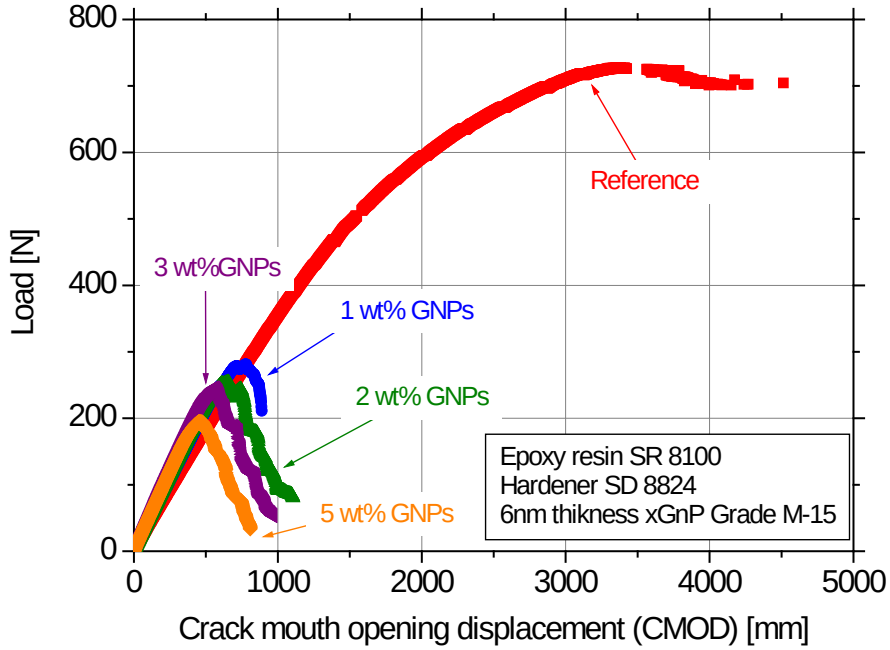

Figure31: Representative curves force - CMOD for resin/GNPs Grade M nanocomposites.

Figure 33 shows the change of the critical stress intensity factor K_{cr} for different concentrations of GNPs. As can be seen in the figure, literature shows that the critical stress intensity factor K_{cr} is increasing up to 1 wt% GNPs concentration while for higher GNPs concentration, K_{cr} decreases, as this is the case for our experimental results. Higher K_{cr} decrease is noticed for the higher GNPs thickness.

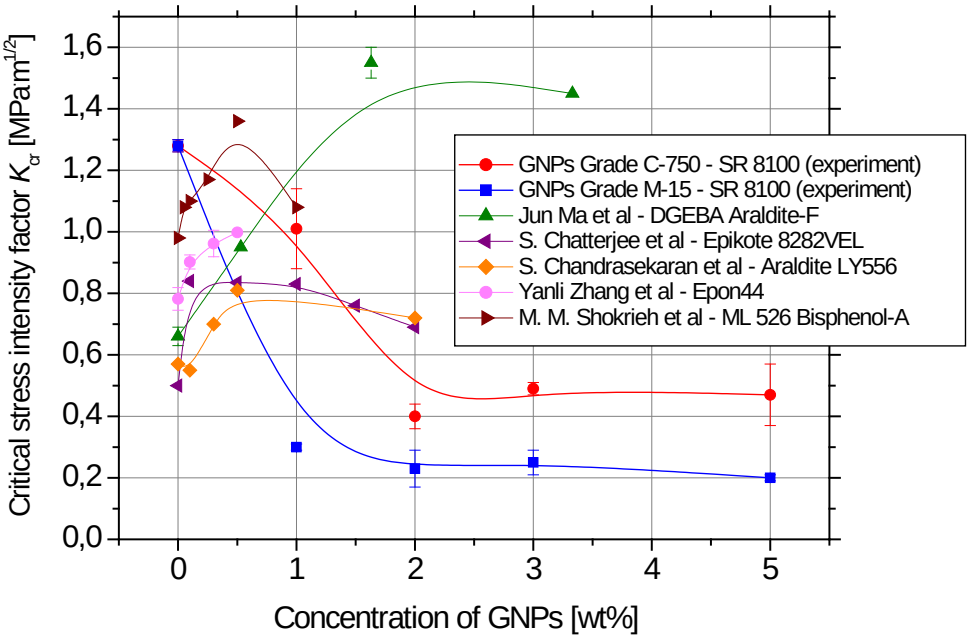

Figure32: Critical stress intensity factor K_{cr} for the different GNPs types and concentrations.

4 RESULTS AND DISCUSSION

This paragraph will try to establish a correlation between the tensile mechanical properties and the critical stress intensity factor for all the conducted experiments of this work. A linear approximation seems to be noticed for the Grade M GNPs between K_{cr} and $R_{p0.2\%}$ while such an approximation couldn't be proposed for the Grade C GNPs. More experiments are needed to get a secure trend of their correlation.

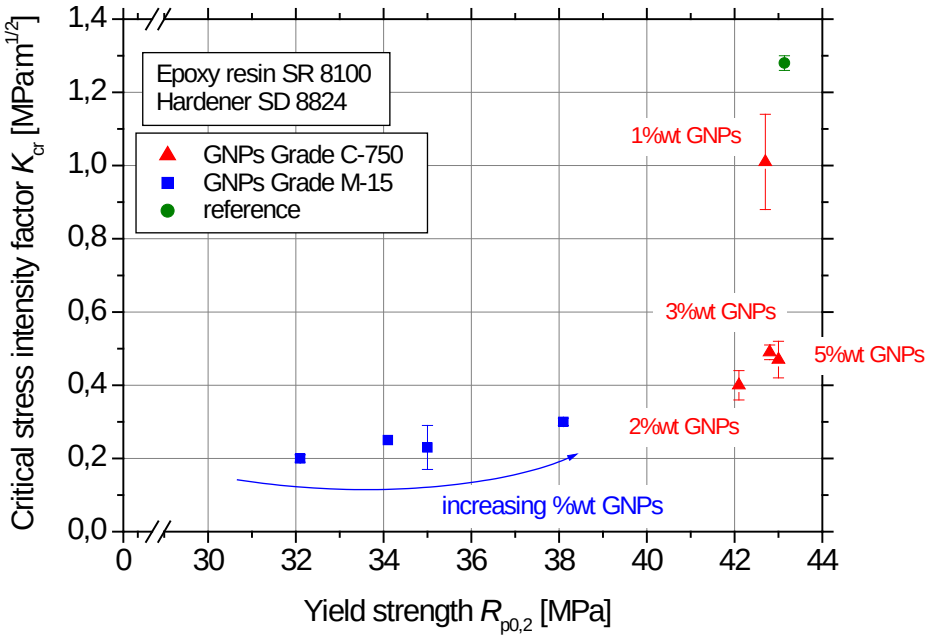

Figure33: The critical stress intensity factor against yield strength for different concentrations and types of GNPs.

Figure 35 shows K_{cr} against A_f which are both continuously decreasing with increasing concentration of Grade M GNPs. A secure conclusion couldn't be drawn for the case of Grade C GNPs. More experiments are needed to get a secure trend of their correlation.

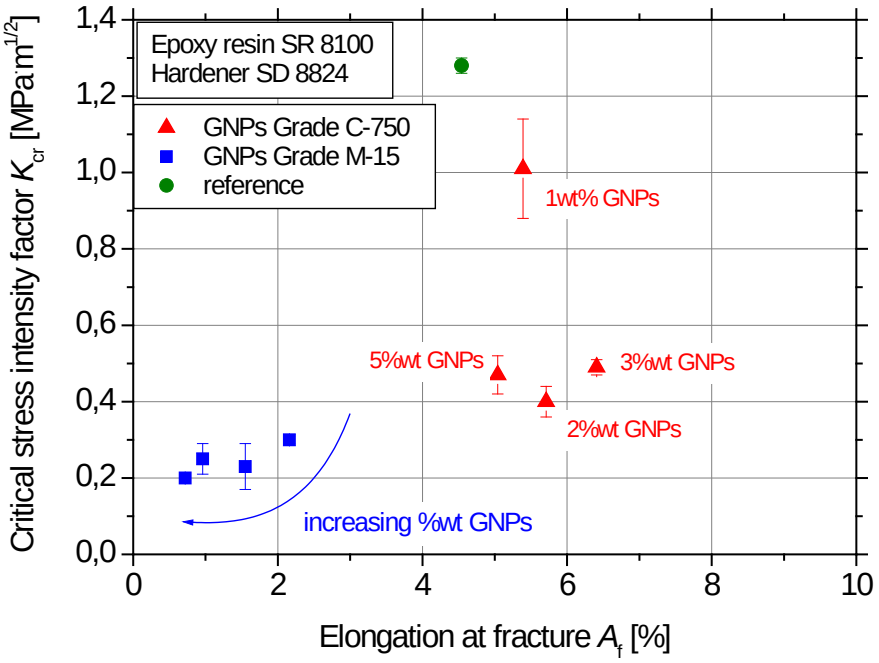

Figure34: .The critical stress intensity factor against elongation at fracture for different concentrations and types of GNPs.

5 CONCLUSIONS

- It is concluded that the filler dispersion, filler size, and the interfacial interactions between The tensile fracture mechanism of the nanocomposites seems to differ with varying GNPs concentration of low thickness (Grade C). For the case of low concentrations (< 1.0 wt% GNPs), increased strength and lower ductility is noticed, while decreased strength and increased ductility is noticed for even higher concentrations (up to 3.0 wt% GNPs). For excess reinforcement (> 5.0 wt% GNPs) a decrease is noticed for all tensile mechanical properties.

- For the case of the addition of GNPs with higher thickness (Grade M), the same mechanisms seems to be the case with the exception of continuous decrease in ductility. This might be attributed to formed porosity during manufacturing of the specimens.

- Critical stress intensity factor K_{cr} decreases with increasing large (> 1.0 wt%) GNPs concentration for both investigated types. Available literature results showed that a small K_{cr} increase should be expected for small (< 1.0 wt%) GNPs concentrations.

6 FUTURE RESEARCH IDEAS

- The influence of the small concentrations (< 1.0 wt%) is already scheduled.
- The effect of mechanical stirring processing time might perhaps be useful to cope with.
- Other types of GNPs (thicker-smaller) might be interesting to investigate their effect on mechanical properties.

7 REFERENCES

[1] Camargo, P.H.C., Satyanarayana, K.G. and Wypych, F., Nanocomposites: Synthesis, Structure, Properties and New Application Opportunities, *Materials Research*, 2009; **12**, pp.1-39.

[2] Webpage http://en.wikipedia.org/wiki/Nanocomposite

[3] Nanocomposites, Nanoparticles, Nanoclays and Nanotubes, Report code: NANO21E, 2006.

[4] S. Baksi, P R Basak & S. Biswas Abstract, NANOCOMPOSITES – TECHNOLOGY TRENDS & APPLICATION POTENTIAL.

[5] http://www.aviation-history.com/theory/composite.htm

[6] E. Gkerou, Thesis, Composite Materials Epoxy Resin Carbon-Fiber-Metallic zinc powders: Construction, Mechanical and Electrical Properties, NTUA School of Chemical Engineering, Athens 2011.

[7] G. Trakakis, Theses, University of Patras, School of Sciences Physics Department "Mechanical Properties of Nanocomposite Materials", Patra 2010, pp.25-26.

[8] N. Tsouvalis, "Engineering Composites" Notes IPPS "Materials Science and Technology", Athens 1998, pp.1-28, 45-50, 68-69.

[9] http://www.phenoxy.com/applications/composites.html

[10] Webpage http://people.bath.ac.uk/ck258/new%20materials%20documents/Engineering%20polymers1.htm

[11] M. Naebe, J. Wang, A. Amini, H. Khayyam, N. Hameed, L.H. Li, Y. Chen & B. Fox, Mechanical Property and Structure of Covalent Functionalised Graphene/Epoxy Nanocomposites, *Scientific Reports*, 2014;**4**, Article number: 4375.

[12] S.G.Prolongo, A. Jimenez-Suarez, R. Moriche, A. Urena, In situ processing of epoxy composites reinforced with graphene nanoplatelets, *Composites Science and Technology* 2013; **86**, pp.185-191.

[13] J. King, Danielle R. Klimek, Ibrahim Miskioglu, Greg M. Odegard, Mechanical Properties of Graphene Nanoplatelet/Epoxy Composites, *Journal of Applied Polymer Science*, 2013; **128**, pp.4217–4223.

[14] http://www.treccani.it/scuola/lezioni/scienze_naturali/chimicagrafene.html

[15] http://www.nanochemistry.it/download/download.html

[16] http://www.graphene-info.com/graphene-products

[17] S. Chatterjee, J.W. Wang, W.S. Kuo, N.H. Tai, C. Salzmann, W.L. Li, R. Hollertz, F.A. Nóesch, B.T.T. Chu, Mechanical reinforcement and thermal conductivity in expanded graphene nanoplatelets reinforced epoxy composites, *Chemical Physics Letters*, 2012; **531**, pp.6-10.

[18] B. Ahmadi-Moghadam, M. Sharafimasooleh, S. Shadlou, F. Taheri. Effect of functionalization of graphene nanoplatelets on the mechanical, *Materials and Design*, 2015; **66**, pp.142–149.

[19] M.-Y. Shen, T.-Y. Chang, T.-H. Hsieh, Y.-L. Li, C. L. Chiang, H. Yang and M.-C. Yip1, Mechanical Properties and Tensile Fatigue of Graphene Nanoplatelets Reinforced Polymer Nanocomposites, *Journal of Nanomaterials*, 2013; 565401.

[20] Q. Meng, J. Jin, R. Wang, H.-C. Kuan, J. Ma, N. Kawashima, A. Michelmore, S. Zhu and C. H. Wang, Processable 3-nm thick graphene platelets of high electrical conductivity and their epoxy composites, *Nanotechnology*,2014; **25** (12) :125707.

[21] W. P. Serena Saw ,M. Mariatti, Properties of synthetic diamond and graphene nanoplatelet-filled epoxy thin film composites for electronic applications, *J Mater Sci: Mater Electron*, 2012; **23**, pp.817–824.

[22] J. Ma,Q. Meng, I. Zaman, S. Zhu, A. Michelmore, N. Kawashima, C. H. Wang, H.-C. Kuan, Development of polymer composites using modified, high-structural integrity graphene

platelets, *Composites Science and Technology*, 2013; **91**, pp.82-91.
[23] S.Chandrasekaran, Christian Seidel, Karl Schulte, Preparation and characterization of graphite nano-platelet (GNP)/epoxy nano-composite: Mechanical, electrical and thermal properties, *European Polymer Journal*, 2013; **49**, pp.3878–3888
[24] Yanli Zhang et al, Tuning the interface of graphene platelets/epoxy composites by the covalent grafting of polybenzimidazole, *Polymer*, 2014; **55**, pp.4990-5000.
[25] MM Shokrieh, M Esmkhani, F Taheri-Behrooz, AR Haghighatkhah, Displacement-controlled flexural bending fatigue behavior of graphene/epoxy nanocomposites, *Journal of Composite Materials*, 2014; **48**, pp.2935–2944.
[26] Fuzhong Wang et al, Mechanical properties and thermal conductivity of graphene nanoplatelet/epoxy composites, *J Mater Sci*, 2015; **50**, pp.1082–1093.
[27] ASTM D 638 Standard Test Method for Tensile Properties of Plastics.
[28] ASTM D 5045 Standard Test Methods for Plane-Strain Fracture Toughness and Strain Energy Release Rate of Plastic Material.
[29] American Society for Testing and Materials (ASTM), *ASTM E8 Standard Test Methods for Tension Testing of Metallic Materials.* ASTM International.
[30] N.D. Alexopoulos, Materials' Strength Notes, University of the Aegean, Chios, 2009.
[31] ASTM E 561 Standard Practice for R-Curve Determination.

FIGURE LIST

TABLE LIST